

FEYNMAN-KAC PATH INTEGRALS AND EXCITED STATES OF QUANTUM SYSTEMS

N.G. Fazleev^{1,2}, J.L. Fry¹, and J.M. Rejcek¹

¹Department of Physics, Box 19059, University of Texas at Arlington,
Arlington, Texas 76019-0059, USA

²Department of Physics, Kazan State University, Kazan, 420008, Russia

ИНТЕГРАЛЫ ПО ТРАЕКТОРИЯМ ФЕЙНМАНА-КАЦА И ВОЗБУЖДЕННЫЕ СОСТОЯНИЯ КВАНТОВЫХ СИСТЕМ

Н.Г. Фазлеев^{1,2}, Дж.Л. Фрай¹, Дж.М. Рейчек¹

¹Университет Техаса в Арлингтоне, Арлингтон, США

²Казанский государственный университет, Казань



*Volume 6, No. 1,
pages 37-49, 2004*

<http://mrsej.ksu.ru>

**FEYNMAN-KAC PATH INTEGRALS AND
EXCITED STATES OF QUANTUM SYSTEMS**

N.G. Fazleev^{1,2}, J.L. Fry¹, and J.M. Rejcek¹

¹*Department of Physics, Box 19059, University of Texas at Arlington,
Arlington, Texas 76019-0059, USA*

²*Department of Physics, Kazan State University, Kazan, 420008, Russia*

We use transformation properties of the irreducible representations of the symmetry group of the Hamiltonian and properties of a continuous path to define a “failure tree” procedure for finding eigenvalues of the Schrödinger equation using stochastic methods. The procedure is used to calculate energies of the lowest excited states of quantum systems possessing anti-symmetric nodal regions in configuration space with the Feynman-Kac path integral method. Within this method, the solution of the imaginary time Schrödinger equation is approximated by random walk simulations on a discrete grid constrained only by symmetry considerations of the Hamiltonian. The required symmetry constraints on random walk simulations are associated with a given irreducible representation of a subgroup of the symmetry group of the Hamiltonian and are found by identifying the eigenvalues for the irreducible representation corresponding to symmetric or antisymmetric eigenfunctions for each group operator. As a consequence, the sign problem for fermions is eliminated. The method provides exact eigenvalues of excited states in the limit of infinitesimal step size and infinite time. The numerical method is applied to compute the eigenvalues of the lowest excited states of the hydrogenic and helium atoms.

I. Introduction

The motivation for the Feynman-Kac path integral formulation comes from the difficulty of defining a measure for the real time Feynman path integral. Feynman's path integral approach to quantum mechanics can be formally described by the expression

$$(e^{-iHt/\hbar}\psi)(\vec{R}_1) = \int_{\Omega(\vec{R}_2;\vec{R}_1)} e^{iA(\omega)/\hbar} \psi(\omega(t)) d\omega \tag{1}$$

where H is the Hamiltonian operator, $\psi(\vec{R}_1)$ is the wave function at the initial time $t = 0$ and position $\omega(0) = \vec{R}_1$, $\Omega(\vec{R}_2; \vec{R}_1) = \{\omega(s) \mid 0 \leq s \leq t, \omega(0) = \vec{R}_1, \omega(t) = \vec{R}_2\}$ denotes the set of all paths starting at \vec{R}_1 and ending at point \vec{R}_2 , $A(\omega)$ is the classical action of the path and $d\omega$ is a measure on $\Omega(\vec{R}_2; \vec{R}_1)$. The notation reads, the time evolution operator $e^{-iHt/\hbar}$ operating on an initial function ψ evaluated at some point \vec{R}_1 is equal to the sum over all paths ω in $\Omega(\vec{R}_2; \vec{R}_1)$, weighted by a function of the action per path and employing some measure $d\omega$. Unfortunately, the path spaces of interest are infinite-dimensional and no Lebesgue-type measure $d\omega$ exists for real $A(\omega)$. Exner [1] states a theorem asserting that the Feynman-type measures cannot exist because the exponential term in Eq. (1) is wildly oscillating unless $A(\omega)$ is purely imaginary. Therefore, the path integrals under consideration denoted by $\int d\omega$ are not integrals in the Lebesgue or Riemann sense. Several approaches [1] have been attempted in order to define meaning to Eq. (1). Most approaches try to bypass this difficulty by defining a suitable class of functions $\psi(\vec{R}_1)$ whose behavior would be smooth enough in some sense to cancel the influence of the oscillations.

One approach to obtaining finite Feynman path integrals involves analytical continuation in time. Consider the Hamiltonian operator $H = -\frac{1}{2}\nabla^2 + V$ and assume that the potential V is continuous. Instead of e^{-iHt} , one may try to get a path integral expression for e^{-tH} . Eq. (1) becomes

$$(e^{-tH}f)(\vec{R}_1) = \int_{\Omega(\vec{R}_2;\vec{R}_1)} \exp\left\{\frac{1}{2} \int_0^t (|\dot{\omega}(s)|^2 - V(\omega(s))) ds\right\} f(\omega) D\omega, \tag{2}$$

where $A(\omega) = \frac{1}{2} \int_0^t (|\dot{\omega}(s)|^2 - V(\omega(s))) ds$ is the action for the Brownian motion path ω and $D\omega$ is a probability measure on the space of all Brownian motion trajectories starting at $\omega(0) = \vec{R}_1$ and ending at $\omega(t) = \vec{R}_2$. The difference between Eq. (1) and Eq. (2) is that the Wiener integrals have a mathematically well-defined measure.

Kac applied Wiener measure to Feynman path integrals to obtain what is now known as the Feynman-Kac formula:

$$(e^{-tH}\psi)(\vec{R}) = \int_{\Omega(\vec{R})} \exp\left(-\int_0^t V(\omega(\tau))d\tau\right) \psi(\omega(t)) d\mu(\omega), \tag{3}$$

where V is the potential in the Hamiltonian operator $H = -\frac{1}{2}\nabla^2 + V$, $\Omega(\vec{R})$ is the set of all continuous paths ω on the interval $[0,t]$ in N dimensional real space \mathfrak{R}^N such that $\omega(0) = \vec{R}$, $\mu(\omega)$ denotes Wiener measure (i.e. a probability measure on the set of all possible trajectories of Brownian motion in \mathfrak{R}^N initially started at position \vec{R}), and ψ is any function which is Lebesgue square integrable, denoted $\psi \in L^2(\mathfrak{R}^N)$. The notation $L^p(\mathfrak{R}^N)$ stands for the set of all functions $f(\vec{r})$ which are Lebesgue measurable on some family of Borel subsets \mathcal{B} of \mathfrak{R}^N and have the property that $\int_B |f|^p d^N r < \infty$ for $1 \leq p \leq \infty$

and $B \in \mathcal{B}$. A rigorous proof of the Feynman-Kac formula and limitations of its application are given by Reed and Simon [2].

The Feynman-Kac formula gives an expected value of a path integral with respect to Wiener measure. If every random path $\omega(t)$ initially begins at some position $\vec{r}_0 = \omega(0)$, the function ψ is defined to be a delta function, $\psi(\omega(0)) = \delta(\omega(0) - \vec{r}_0)$. Substituting this into Eq. (3) yields

$$\bar{S}(t, \vec{r}_0) \equiv E_{\vec{r}_0} \left[\exp\left(-\int_0^t V(\omega(\tau))d\tau\right) \right], \tag{4}$$

where $E_{\vec{r}_0}(\cdot)$ is the expected value of the Wiener integral with $\vec{r}_0 = \omega(0)$ the initial position of a Wiener process (Brownian motion).

The Feynman-Kac path integral method was first applied in finding the ground state energy of a one-dimensional physical system by Donsker and Kac [3]. It has been generalized for dimensions $N > 1$ for a large class of potential functions [4] including those potentials with $|\vec{r}|^{-1}$ singularities (for example the Coulomb potential). The exact solution for the ground state eigenvalue may be written

$$\lambda_1 = \lim_{t \rightarrow \infty} \left(-\frac{1}{t} \ln [\bar{S}(t, \vec{r}_0)] \right) = \inf \left\{ \int_{\Omega_0} V(\vec{r}) \varphi^2(\vec{r}) d^N r + \frac{1}{2} \int_{\Omega_0} \langle \nabla \varphi(\vec{r}), \nabla \varphi(\vec{r}) \rangle d^N r \right\}, \quad (5)$$

where $\nabla = \left(\frac{\partial}{\partial r_1}, \frac{\partial}{\partial r_2}, \dots, \frac{\partial}{\partial r_N} \right)$ is the gradient and $\langle \cdot \rangle$ is the scalar product in some region contained in an N-dimensional real configuration space, $\Omega_0 \subset \mathfrak{R}^N$.

The Feynman-Kac path integral method has been used in more recent literature [5,6] to calculate the ground state energies of several atomic and exactly solvable quantum systems. The solutions for the ground state eigenvalues were approximated by random walk simulations on a discrete grid, based on the Donsker-Varadhan invariance principle [7] for Brownian motion. The method provides exact ground state eigenvalues in the limit of infinitesimal step size and infinite time.

A desired extension of the method is application to excited states of quantum systems. For a given Hamiltonian H , which describes a quantum system, if additional constraints were added requiring random walk simulations on a discrete grid to remain confined in a configuration space region the bounds of which coincide with the zeroes of an excited eigenstate, called a nodal region, the Feynman-Kac method would converge to the eigenvalue of that eigenstate. However, for most quantum systems, one does not know where the eigenfunction changes from positive to negative. This is related to the sign problem in stochastic methods. A useful approximation is the fixed-node approximation, where a trial function with known nodal regions is used to approximate the exact eigenfunction. If the trial function nodes exactly correspond to the true eigenfunction nodes, then the exact eigenvalue can be calculated. A survey of different stochastic methods used to solve the Schrödinger equation for many body systems is given in [8-10].

In this paper we show that for quantum systems possessing particular symmetries in configuration space, it is possible to use representation theory of finite groups and properties of the continuous path to develop constraints on the random walk in order to compute the lowest energy of a state that transforms according to a chosen irreducible representation of the invariant group of the Hamiltonian within the Feynman-Kac path integral method. These constraints are incorporated into a procedure called the “failure tree” method. In Section II we present precise definitions of a nodal region and a continuous path as well as several theorems related to properties of eigenstates associated with a nodal region. In Section III we introduce the “failure trees” and describe how they are implemented. In Section IV we present several theorems from representation theory of finite groups and use them to define the “failure trees”. In Section V we describe how symmetry considerations are applied in the creation of “failure trees” and present the results of numerical calculations for excited states of the hydrogenic and helium atoms. Conclusions are presented in Section VI.

II. Properties of bounded regions of configuration space

For further consideration, a few definitions and properties related to the continuity of a path in configuration space will be needed. Given two separate points \vec{R}_1 and \vec{R}_2 in N-dimensional space \mathfrak{R}^N , for every continuous path $P(\vec{R}_1, \vec{R}_2)$ connecting the points there exists at least one set of one dimensional continuous parametric functions $f_1(\vec{R}_1, \vec{R}_2, t), f_2(\vec{R}_1, \vec{R}_2, t), \dots, f_N(\vec{R}_1, \vec{R}_2, t)$ Ω_n , with the parameter t , $[0 \leq t \leq T]$, so that the path can be represented by the set of points

$$P(\vec{R}_1, \vec{R}_2) \equiv \left\{ \vec{R} \in \mathfrak{R}^N \left| \vec{R} = \begin{matrix} f_1(\vec{R}_1, \vec{R}_2, t) & f_1(\vec{R}_1, \vec{R}_2, 0) & f_1(\vec{R}_1, \vec{R}_2, T) \\ f_2(\vec{R}_1, \vec{R}_2, t) & f_2(\vec{R}_1, \vec{R}_2, 0) & f_2(\vec{R}_1, \vec{R}_2, T) \\ \vdots & \vdots & \vdots \\ f_N(\vec{R}_1, \vec{R}_2, t) & f_N(\vec{R}_1, \vec{R}_2, 0) & f_N(\vec{R}_1, \vec{R}_2, T) \end{matrix} \text{ with } \vec{R} = f_1(\vec{R}_1, \vec{R}_2, 0) \text{ and } \vec{R}_2 = f_1(\vec{R}_1, \vec{R}_2, T) \right. \right\} \quad (6)$$

In general, there may be an infinite number of different continuous paths between \vec{R}_1 and \vec{R}_2 .

Consider a physical system defined by a Hamiltonian $H = -\frac{1}{2} \nabla^2 + V$ on a configuration space region $\Omega_0 \subseteq \mathfrak{R}^N$, which has a boundary $\partial\Omega_0$ that defines the limits of the system. It has been shown by Ray [11] that there exists a set of eigenfunctions $\{\psi_n(\vec{R})\}$ on Ω_0 such that $H\psi_n(\vec{R}) = \lambda_n \psi_n(\vec{R})$ and $\psi_n(\vec{R}) = 0$ on $\vec{R} \in \partial\Omega_0$. A nodal region Ω_m is a connected sub-region $\Omega_m \subseteq \Omega_0$ with bound $\partial\Omega_m$ defined as the set of points \vec{R} , where $\psi_m(\vec{R}) = 0$, which are called the nodes of the eigenfunction. By connected it is meant that for every two separate points in the nodal region, $\vec{R}_1, \vec{R}_2 \in \Omega_m$, there exists at least one continuous path between them contained in the nodal region that does not contain any boundary point. This implies there are no internal nodal regions that divide Ω_m into smaller sub-regions. Given an eigenfunction $\psi_m(\vec{R})$, the entire open set Ω_0 can be decomposed into a countable set of disjoint connected nodal regions $\{\Omega_m(\vec{R}_i)\}$.

Some characteristics of nodal regions for fermion systems have been explored in [12-15]. A few properties of the eigenfunctions and their nodal regions are described by the following three theorems. Proofs of the theorems are given elsewhere [16-18].

Theorem 1. The ground state $\psi_1(\vec{R})$ and only the ground state of a quantum system described by the Hamiltonian H has no internal nodes.

Theorem 2. Application of the Feynman-Kac method to any nodal region consistent with an eigenfunction $\psi_m(\vec{R})$ of the Hamiltonian will produce the eigenvalue λ_m of that state.

Theorem 3. If any nodal region Ω_m of an eigenfunction $\psi_m(\vec{R})$ is entirely contained in any nodal region Ω_n of another eigenfunction $\psi_n(\vec{R})$, then the corresponding eigenvalue λ_m is greater than or equal to λ_n : $\Omega_m \subset \Omega_n \Rightarrow \lambda_m \geq \lambda_n$. It follows from the properties described by theorems 1-3, that if one can confine a random walk to a closed bounded region in configuration space that coincides with the zeros of the m th excited state of the quantum system under consideration, the corresponding eigenvalue λ_m can be calculated using the Feynman-Kac method. Thus, the fundamental problem is to devise a random walk that starts and remains in this region throughout the entire walk. It will be shown below that this can be done for some physical systems by taking into consideration symmetry properties of the Hamiltonian in configuration space and properties of a continuous path.

III. Introduction of the “failure trees”

Let θ represent a configuration space operator such as rotation, permutation or inversion, which takes a $3N$ -dimensional position vector $\vec{R}_1 \equiv (x_1, y_1, z_1, x_2, \dots, z_N)$ and transforms it to another vector $\theta^{-1}\vec{R}_1 \equiv (x'_1, y'_1, z'_1, x'_2, \dots, z'_N)$. If a Hamiltonian remains invariant to θ , then it is said that the system possesses symmetry with respect to θ and this implies the operation commutes with the Hamiltonian, $[H, \theta] = 0$. For every operator θ that commutes with the Hamiltonian and for every eigenfunction $\psi_n(\vec{R})$ of H , it is also true that $H\theta\psi_n(\vec{R}) = \lambda_n\theta\psi_n(\vec{R})$. That is, $\theta\psi_n(\vec{R})$ is also an eigenfunction of H with the degenerate eigenvalue λ_n . If $\theta\psi_m(\vec{R}) = c_m\psi_m(\vec{R})$ and $c_m < 0$, and if $\psi_m(\vec{R})$ is continuous in the full configuration space Ω_0 containing \vec{R} and $\theta^{-1}\vec{R}$, then there must be some position \vec{R}' where $\psi_m(\vec{R}') = 0$. This implies that at least one node exists for continuous $\psi_m(\vec{R})$.

Define a nodal region $\Omega_m(\vec{R}_1)$ around a point \vec{R}_1 , that belongs to the full configuration space Ω_0 as the largest connected open subregion of points $\{\vec{R}\}$ that can be reached from \vec{R}_1 such that $\vec{R} \in \Omega_m(\vec{R}_1)$ implies $\theta^{-1}\vec{R} \notin \Omega_m(\vec{R}_1)$. Configuration space is then divided into two disjoint subsets, $\Omega_m(\vec{R}_1)$ and $\Omega_0 - \Omega_m(\vec{R}_1)$ respectively, and every continuous path $P(\vec{R}, \theta^{-1}\vec{R})$ must cross a nodal surface. From the set of all possible continuous paths from a point \vec{R}_1 to $\vec{R}_2 \in \Omega_m(\vec{R}_1)$, every path that remains interior to the nodal region, denoted $P(\vec{R}_1, \vec{R}_2) \subset \Omega_m$, requires that every $\vec{R} \in P(\vec{R}_1, \vec{R}_2)$ implies $\theta^{-1}\vec{R} \notin P(\vec{R}_1, \vec{R}_2)$. All paths that meet this requirement are interior to the nodal region. All paths that do not meet this requirement contain a continuous subpath $P(\vec{R}, \theta^{-1}\vec{R})$ as part of the full path $P(\vec{R}_1, \vec{R}_2)$ that leaves the nodal region.

In general, the condition that a point $\theta^{-1}\vec{R}$ is not included in a path must be checked at each step in a random walk numerical simulation for each and every point \vec{R} contained in the path. If any such point $\theta^{-1}\vec{R}$ is found, the path has left the nodal region and must be assigned a numerical weight of zero. Otherwise, the path is fully contained in the nodal region and provides a nonzero contribution to the Feynman-Kac path integral. For many Hamiltonians there are configuration space operators θ that possess symmetry relations that can be utilized along with continuity properties of a path to simplify the procedure of checking each step in a random walk simulation. The procedure used in this paper to check the condition that a point $\theta^{-1}\vec{R}$ is not included in a path is called the “failure tree” method and is described in the following paragraphs.

In order to determine whether a numerically simulated path remains interior to a nodal region we utilize the definition of a continuous path given above. According to Eq. (6) the existence of a subpath $P(\vec{R}, \theta^{-1}\vec{R})$ implies that it can be represented by at least one set of one-dimensional continuous parametric functions $\{f_i(\vec{R}, \theta^{-1}\vec{R}, t), i = 1, 2, 3 \dots N\}$, with the parameter t , $[0 \leq t \leq T]$. As the random walk path is traced out in a numerical simulation, its representation by all parametric functions $f_i(\vec{R}, \theta^{-1}\vec{R}, t)$ must be checked. When a single parametric function is found to represent the set of points of the simulated path $P(\vec{R}, \theta^{-1}\vec{R})$, the path is still interior to the nodal region because the other $N-1$ parametric functions do not represent the path. It is only necessary to assign zero contribution from the path when all N parametric functions have are shown to represent the simulated path. This process can be graphically represented using a “failure tree” as shown in Fig. 1.

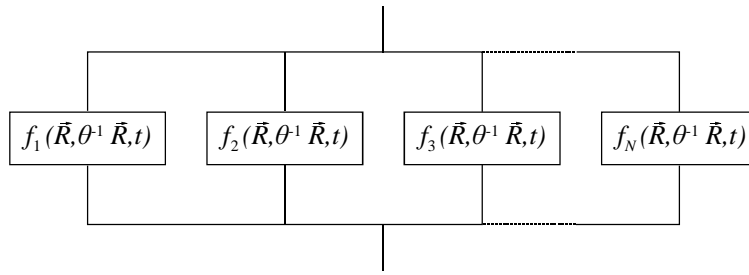


Fig. 1. Illustration of a failure tree

The figure can be understood as two points (top and bottom) connected by N parallel switches. The nonexistence of $f_i(\vec{R}, \theta^{-1} \vec{R}, t)$ is represented by the switch turned “on” and the existence of $f_i(\vec{R}, \theta^{-1} \vec{R}, t)$ by the switch turned “off”. Thus, finding that the j -th condition $f_j(\vec{R}, \theta^{-1} \vec{R}, t)$ does occur turns off one switch, yet the tree still connects the top to the bottom of the graph. Only after all switches are turned off is the connection broken. Likewise, if all $f_i(\vec{R}, \theta^{-1} \vec{R}, t)$ are found to represent the path, the necessary conditions have been demonstrated for the existence of a continuous path between two points \vec{R} and $\theta^{-1} \vec{R}$.

IV. Application of group theory

Group theory considerations can be used to define the necessary symmetry constraints for construction of “failure trees” that allow selection of random walk paths that do not leave a configuration space region $\Omega_m(\vec{R})$. Consider a set of coordinate transformations that commute with the Hamiltonian and form a group \mathcal{G} with elements θ . We can define a projection operator $\mathcal{P}_{\Gamma_m}^q$ for the irreducible representations of the group by

$$\mathcal{P}_{\Gamma_m}^q = \frac{d_g}{O_G} \sum_{j=1}^{O_G} \Gamma_{lm}^{q*}(\theta_j) \theta_j, \quad (7)$$

where Γ_{lm}^q is the m th row and n th column of the q -th irreducible representation of the element θ , d_g is the dimension of the irreducible representation and O_G the order of the group. The projection operator can be used to project out eigenfunctions that possess the symmetry of a given irreducible representation Γ^q .

In the remainder of this paper we will consider one-dimensional irreducible representations, all of which possess properties described by the following theorems, which can be easily proved from the definition of the projection operator [19,20].

Theorem 4. All operators θ_j of the group \mathcal{G} commute with every projection operator of all one-dimensional irreducible representations: $[\mathcal{P}_{\Gamma_m}^q, \theta_j] = 0 \forall \theta_j \in \mathcal{G}$.

Theorem 5. Given an arbitrary function f , the q -th projection from a one-dimensional irreducible representation: $[\mathcal{P}_{\Gamma_m}^q, \theta_j] = 0 \Rightarrow \theta_j g_{\Gamma_m}^q = c_i g_{\Gamma_m}^q$, where $g^q \neq 0$, is an eigenfunction of all operators θ_j of the group with eigenvalue $1/\Gamma^{q*}(\theta_i)$, $\theta_i g^q = \{1/\Gamma^{q*}(\theta_i)\} g^q$ for all θ_j in \mathcal{G} and all q .

Theorem 6. Every one-dimensional irreducible representation Γ^q is uniquely defined by the eigenvalues $\{1/\Gamma^{q*}(\theta_i)\}$ of the elements $\{\theta_j\}$ of group \mathcal{G} .

As shown in Theorem 6, since every nonzero projection of a function $g^q = \mathcal{P}^q f$ is an eigenfunction of each operator θ , there is a unique set of eigenvalues $\{1/\Gamma^{q*}(\theta_i)\}$ that describes each irreducible representation. The required symmetry properties associated with a given irreducible representation can be found by identifying the eigenvalues $\{1/\Gamma^{q*}(\theta_i)\}$ as being either ± 1 , corresponding to symmetric or antisymmetric eigenfunctions.

We note that every nonzero projection made on an eigenfunction of the Hamiltonian $g^q = \mathcal{P}^q \psi_m(\vec{R})$ remains an eigenfunction of the Hamiltonian. This is due to the fact that $[H, \theta_i] = 0$, which implies $[H, \sum b_i \theta_i] = 0$ for all constants b_i . Since the projection g^q must satisfy the symmetry properties of the irreducible representation Γ^q , g^q must possess all symmetry nodes associated with Γ^q . The relevant symmetry property (antisymmetry) is identified by finding the subset of operators $\{\theta_j\}$ such that $\theta_j g^q = -g^q$.

Using this antisymmetry property for the q th irreducible representation, it is possible to construct “failure trees” in order to select random walk paths that do not violate the symmetry requirements of the projected eigenfunction $\mathcal{P}^q \psi_m(\vec{R})$. The only constraints imposed on a random walk are defined from the symmetry requirements for the

irreducible representation. It follows from Theorem 2 that application of the Feynman-Kac method will produce the lowest energy of a state that transforms according to that irreducible representation.

V. Applications of the “failure tree” method

a. Hydrogenic *p* and *d* excited states

Consider the hydrogenic atom described as a single particle with elementary charge and mass *M* moving in a three-dimensional Coulomb potential defined as $V(\vec{r}) = -Zke^2/|\vec{r}|$, where *Z* is an integer, *k* is the Coulomb constant and *e* is the electron charge. Since the Weiner integral is usually numerically simulated in Cartesian coordinates, the Schrödinger equation, symmetry operations and the eigenfunctions are defined in terms of Cartesian coordinates. The Schrödinger equation for the system can be written as

$$\left[-\frac{1}{2}\nabla^2(\vec{r}) - \frac{Z}{|\vec{r}|} \right] \psi(\vec{r}) = \lambda\psi(\vec{r}), \tag{8}$$

with the unit of energy $U = \hbar^2 / Ms^2$ and $s = \hbar^2 / Mke^2$ the unit of length. The eigenfunctions are known exactly and can be expressed in terms of the cubic harmonics. By inspection of the Schrödinger equation, it can be seen that there are many symmetry operators, which leave the equation invariant. One is free at this point to choose operators that form a large number of possible subgroups, each possessing unique symmetry properties. The four configuration space operations $[E, \theta_2, \theta_3, \theta_4]$ defined by

$$\begin{aligned} E\psi(x, y, z) &= \psi(x, y, z) \\ \theta_2\psi(x, y, z) &= \psi(-x, y, z) \\ \theta_3\psi(x, y, z) &= \psi(x, -y, -z) \\ \theta_4\psi(x, y, z) &= \psi(-x, -y, -z) \end{aligned}$$

leave the Hamiltonian invariant and form a group G_1 . The multiplication table and irreducible representations for the group are shown in Table I.

Table I. *The multiplication table and the irreducible representations for the group G_1 (the hydrogenic atom)*

	<i>E</i>	θ_2	θ_3	θ_4		<i>E</i>	θ_2	θ_3	θ_4
<i>E</i>	<i>E</i>	θ_2	θ_3	θ_4	Γ^1	1	1	1	1
θ_2	θ_2	<i>E</i>	θ_4	θ_3	Γ^2	1	1	-1	-1
θ_3	θ_3	θ_4	<i>E</i>	θ_2	Γ^3	1	-1	1	-1
θ_4	θ_4	θ_3	θ_2	<i>E</i>	Γ^4	1	-1	-1	1

Given any subgroup of the Hamiltonian, its symmetry properties can be used to generate solutions that are either eigenfunctions of the Hamiltonian or linear combinations of degenerate eigenfunctions of the Hamiltonian. In the absence of specific knowledge of the eigenstates of the Hamiltonian, compatibility tables could be used to identify possible relationships with the irreducible representations of the full group. By using the projection operators defined in Eq. (7), it is possible to project out of the eigenfunctions of the Hamiltonian of the hydrogenic atom new eigenfunctions with the symmetry of the *q*-th irreducible representation Γ^q defined in Table I. The first few projected eigenfunctions for each irreducible representation are shown in Table II. Note that the hydrogenic spectrum has been sorted and classified by the irreducible representations of G_1 .

Table II. *Classification of the first few eigenfunctions for the group G_1 (the hydrogenic atom)*

	Γ^1	Γ^2	Γ^3	Γ^4
λ_1	$\Psi_{1s}(\vec{r})$			
λ_2	$\Psi_{2s}(\vec{r})$	$\Psi_{2p_y}(\vec{r})$	$\Psi_{2p_x}(\vec{r})$	
		$\Psi_{2p_z}(\vec{r})$		
λ_3	$\Psi_{3s}(\vec{r})$	$\Psi_{3p_y}(\vec{r})$	$\Psi_{3p_x}(\vec{r})$	$\Psi_{3d_{xy}}(\vec{r})$
	$\Psi_{3d_{yz}}(\vec{r})$	$\Psi_{3p_z}(\vec{r})$		$\Psi_{3d_{xz}}(\vec{r})$
	$\Psi_{3d_{x^2-y^2}}(\vec{r})$			
	$\Psi_{3d_{3z^2-r^2}}(\vec{r})$			

If another subgroup were constructed using a different set of operators with the property $[H, \theta_i] = 0$, the entire spectrum could be reclassified by the new irreducible representations. For example, the subgroup G_2 defined by

$$\begin{aligned}
 E\psi(x, y, z) &= \psi(x, y, z) \\
 \theta_3\psi(x, y, z) &= \psi(x, -y, z) \\
 \theta_6\psi(x, y, z) &= \psi(x, y, -z) \\
 \theta_3\psi(x, y, z) &= \psi(x, -y, -z)
 \end{aligned}$$

also forms a group that is isomorphic to G_1 , but the hydrogenic spectrum would be reclassified based on the new irreducible representations. The particular choice of subgroup G_1 above allows the classification of the hydrogenic spectrum in such a way that p and d eigenstates belong to different irreducible representations.

The symmetry properties for each irreducible representation can be deduced by deriving the eigenvalue for every operator of the group. This will reveal the symmetric and antisymmetric properties of the projected wavefunctions $\mathcal{P}^i\psi_m(\vec{R})$ that transform like a particular irreducible representation Γ^q as stated in Theorem 6. The symmetry properties of the Γ^2 irreducible representation can be determined by using all four operators of the group as follows. Let $g_2(x, y) \equiv \mathcal{P}^2 f(x, y) = \frac{1}{4}[E + \theta_2 - \theta_3 - \theta_4]f(x, y)$. Then the symmetry properties of $g_2(x, y)$ are determined as

$$\begin{aligned}
 \theta_2 g_2(x, y) &= \theta_2 \frac{1}{4}[E + \theta_2 - \theta_3 - \theta_4]f(x, y) = \\
 &= \frac{1}{4}[\theta_2 + E - \theta_4 - \theta_3]f(x, y) = +g_2(x, y) \\
 \theta_3 g_2(x, y) &= \theta_3 \frac{1}{4}[E + \theta_2 - \theta_3 - \theta_4]f(x, y) = \\
 &= \frac{1}{4}[\theta_3 + \theta_4 - E - \theta_2]f(x, y) = -g_2(x, y) \\
 \theta_4 g_2(x, y) &= \theta_4 \frac{1}{4}[E + \theta_2 - \theta_3 - \theta_4]f(x, y) = \\
 &= \frac{1}{4}[\theta_4 + \theta_3 - \theta_2 - E]f(x, y) = -g_2(x, y)
 \end{aligned} \tag{9}$$

Eq. (9) shows that every function belonging to Γ^2 must be symmetric with respect to θ_2 and antisymmetric with respect to operators θ_3 and θ_4 . The antisymmetric conditions are used to define the particular symmetry constraints on a random walk associated with Γ^2 symmetry. The corresponding “failure tree” is shown in Fig. 2 along with the “failure trees” associated with Γ^3 and Γ^4 . The notation θ_i is used to denote all “failure tree” conditions associated with each operator θ_i as described in Section III.

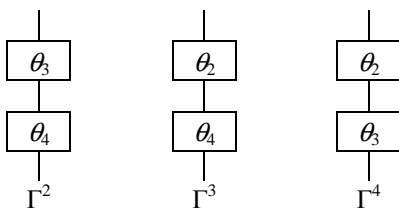


Fig. 2. The failure trees for group G_1

By this procedure, it is assured that every path that does not fail the symmetry constraints defined by Γ^2 belongs to a configuration space region with that symmetry. Using Eq. (5) and Theorem 2, of all possible configuration space regions consistent with the symmetry constraints, in the limit of large t , the Feynman-Kac method assures convergence to the lowest energy of the eigenstate with Γ^2 symmetry.

The task of checking each point \vec{R} in a given path in order to find if $\theta^{-1}\vec{R}$ is also in the path can be significantly simplified for many configuration space operators using “failure tree” conditions as described in Section III above. The “failure tree” conditions associated with operators θ_2 , θ_3 and θ_4 defined in Table I are described as follows. For every continuous path between $\vec{R} = (x, y, z,)$ and $\theta_2^{-1}\vec{R} = (-x, y, z)$, it is necessary that there exist continuous functions $f_i(\vec{R}, \theta_2^{-1}\vec{R}, t)$ such that the following conditions hold true

$$\begin{aligned}
 f_1(\vec{R}, \theta_2^{-1}\vec{R}, t) &= f_1(\vec{R}, \theta_2^{-1}\vec{R}, 0) = x \ \& \ f_1(\vec{R}, \theta_2^{-1}\vec{R}, T) = -x \\
 f_2(\vec{R}, \theta_2^{-1}\vec{R}, t) &= f_2(\vec{R}, \theta_2^{-1}\vec{R}, 0) = y \ \& \ f_2(\vec{R}, \theta_2^{-1}\vec{R}, T) = y \\
 f_3(\vec{R}, \theta_2^{-1}\vec{R}, t) &= f_3(\vec{R}, \theta_2^{-1}\vec{R}, 0) = z \ \& \ f_3(\vec{R}, \theta_2^{-1}\vec{R}, T) = z
 \end{aligned}$$

For f_1 , this implies there is some $t = t'$ such that $x = f(\vec{R}, \theta^{-1}\vec{R}, t') = 0$. This means that a necessary condition to move from \vec{R} to $\theta^{-1}\vec{R}$ is for the path to pass through $x = 0$. This is also a sufficient condition for a path to fail the antisymmetric requirement associated with operator θ_2 since every point $\vec{R} = (0, y, z) = \theta_2^{-1}\vec{R}$. This antisymmetric requirement represents the yz plane at $x = 0$. Therefore, in order to assure that no continuous path between \vec{R} and $\theta^{-1}\vec{R}$ is included in a simulation, it is both necessary and sufficient to require that every path does not cross the yz plane at $x = 0$. In order to keep this condition associated with operator θ_2 independent of where the path begins, the sign of the product of the parametric functions at the initial x_0 and the current x value,

$xx_0 = f_1(\vec{R}_0, \vec{R}, t) f_1(\vec{R}_0, \vec{R}, 0)$, must be checked. Then, no matter what initial value is used, the condition $x = 0$ means the path has failed the antisymmetric requirement associated with operator θ_2 . The resulting “failure tree” is illustrated in Fig. 3a.

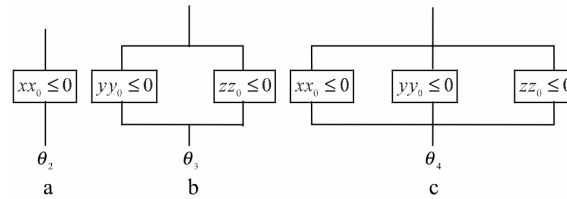


Fig. 3. The failure trees associated with operators θ_2 , θ_3 and θ_4

The “failure tree” conditions for operator θ_3 are described as follows. For every continuous path between \vec{R} and $\theta_3^{-1}\vec{R} = (x, -y, -z)$, it is necessary that continuous functions $f_i(\vec{R}, \theta_3^{-1}\vec{R}, t)$ be generated such that

$$\begin{aligned} f_1(\vec{R}, \theta_3^{-1}\vec{R}, t) &= f_1(\vec{R}, \theta_3^{-1}\vec{R}, 0) = x \ \& \ f_1(\vec{R}, \theta_3^{-1}\vec{R}, T) = x \\ f_2(\vec{R}, \theta_3^{-1}\vec{R}, t) &\ni f_2(\vec{R}, \theta_3^{-1}\vec{R}, 0) = y \ \& \ f_2(\vec{R}, \theta_3^{-1}\vec{R}, T) = -y . \\ f_3(\vec{R}, \theta_3^{-1}\vec{R}, t) &= f_3(\vec{R}, \theta_3^{-1}\vec{R}, 0) = z \ \& \ f_3(\vec{R}, \theta_3^{-1}\vec{R}, T) = -z \end{aligned}$$

For f_2 and f_3 , this implies there is some $t = t'$ and $t = t''$ such that $y = f_2(\vec{R}, \theta_3^{-1}\vec{R}, t') = 0$ and $z = f_3(\vec{R}, \theta_3^{-1}\vec{R}, t'') = 0$. Therefore a necessary condition for a path to fail the antisymmetric requirement associated with operator θ_3 is to include in the path any points $\vec{R} = (x, 0, z)$ and $\vec{R} = (x, y, 0)$. This represents a path crossing the xy plane at $z = 0$ and the xz plane at $y = 0$. The resulting “failure tree” is illustrated in Fig. 3b. This is also a sufficient condition for a path to fail the antisymmetric requirement of operator θ_3 . Since the reflection symmetry operators across the xy and xz planes also commute with the Hamiltonian for the hydrogenic system as shown in the group G_2 defined above, all eigenfunctions of the Hamiltonian that are antisymmetric to operator θ_3 must either be antisymmetric to θ_5 or θ_6 , or a degenerate eigenstate can be projected out that does have this same antisymmetric property. Failing the constraints defined for both θ_5 and θ_6 produces the same “failure tree” that is defined for θ_3 . Therefore the “failure tree” in Fig. 3b is both a necessary and sufficient condition to describe the antisymmetric requirements associated with operator θ_3 . Note that if the reflection operators θ_5 and θ_6 do not commute with a given Hamiltonian, the “failure tree” in Fig. 3b would only be a necessary condition for a path to remain consistent with θ_3 symmetry and further checks would be needed to determine if a path has failed the symmetry conditions for θ_3 . Using the same procedure as described above, the necessary and sufficient conditions associated with operator θ_4 were derived and are shown in Fig. 3c.

Using the requirements associated with these operators, the “failure trees” for the irreducible representations defined in Fig. 2 can be simplified because of the redundant symmetry properties associated with the operators. For example, letting $A = [xx_0 \leq 0]$, $B = [yy_0 \leq 0]$, $C = [zz_0 \leq 0]$ and using the property $[A \cup (A \cap B)] = A$, the Boolean logic for the Γ^2 “failure tree” reduces to $(B \cap C) \cup [A \cup (B \cap C)] = (B \cap C)$, as illustrated in Fig. 4.

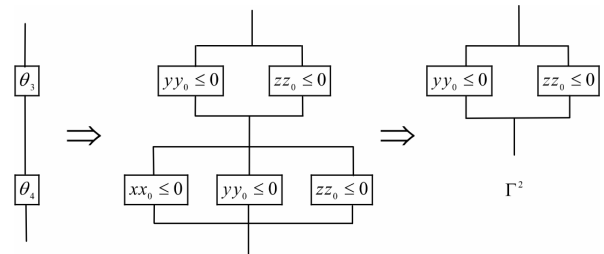


Fig. 4. The failure tree for Γ^2 symmetry

The resulting “failure tree” constraints associated with Γ^3 and Γ^4 irreducible representations are shown in Fig. 5. Note that any function belonging to Γ^1 must be symmetric with respect to every operator in the group. This implies every function belonging to Γ^1 is fully symmetric and therefore no “failure tree” will exist for the Γ^1 irreducible representation. This further implies that the ground state will belong to Γ^1 .

Consider a random walk numerical simulation to the solution of the Schrödinger equation of the hydrogenic atom Eq. (8), using the Feynman-Kac method as described in [6]. The calculation of the lowest energy belonging to Γ^2 (which is an excited state to the system and also degenerate to the eigenvalue corresponding to the lowest eigenstate belonging to Γ^3) is performed by random walk simulations of Eq. (8) with the imposed “failure tree” constraints defined in Fig. 5. No explicit knowledge of the nodal structure is used in this calculation. As noted earlier, the implementation of the “failure tree” constraints in the simulation will restrict the random walk to the regions where the wavefunction does not change sign.

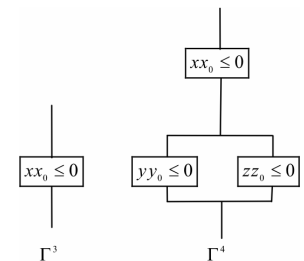


Fig. 5. The failure trees for Γ^3 and Γ^4 symmetry

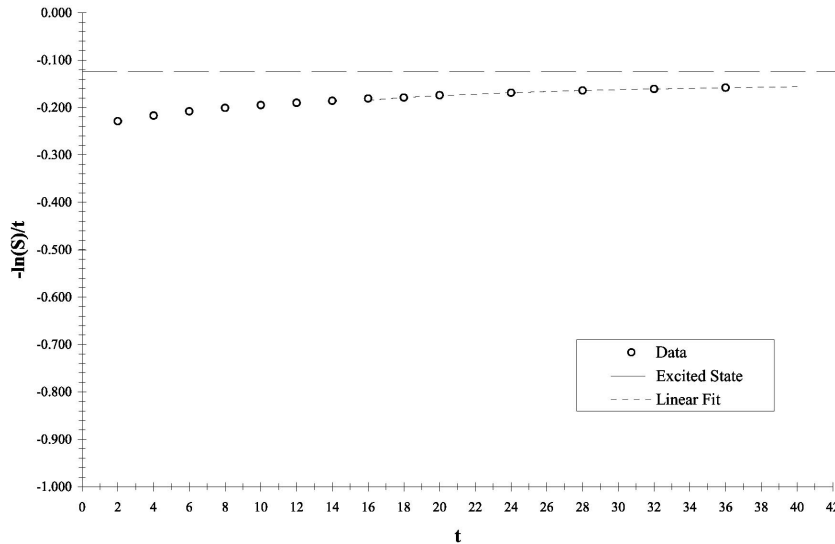


Fig. 6. Plot of $-\ln[\bar{S}(t, \vec{r}_0)]/t$ versus t for the hydrogen $2p_y$ excited state

Fig. 6 shows a plot of $-\ln[\bar{S}(t, \vec{r}_0)]/t$ versus t including 1σ error bars for the uncertainty, where $\bar{S}(t, \vec{r}_0)$ is the path integral simulation result as defined in [6]. The initial position for each random walk was set at $r_0 = \frac{3}{7}(\hat{i} - \hat{j} + \hat{k})$ and the step size $\Delta r = (\Delta x, \Delta y, \Delta z)$ is determined to be $\Delta x = \Delta y = \Delta z = s/\sqrt{n}$, where $n = 900$ and s and U are defined in Eq. (8). Note that the error bars are so small for this calculation that they do not appear. Five million paths were needed for this convergence. A least squares fit of the data starting at $t = 28$ to the equation

$$-\ln[\bar{S}(t, x_0)]/t = \lambda_1 - \ln[C_1]/t \tag{10}$$

is shown along with the exact eigenvalue. The least square fit yields the values $\ln[C_1] = -0.762(60)Ut$ and $\lambda_{2p_y} = -0.1377(12)U$, where the parentheses denote the uncertainty in the final two significant figures. This compares with the lowest eigenvalue $\lambda_{2p_y} = -(1/8)U = -0.125U$ for Γ^2 irreducible representation. The difference between the exact result and the numerical calculation is attributed to the finite step size and time used in the calculation. Decreasing the step size Δr and increasing t would result in closer convergence to the exact eigenvalue.

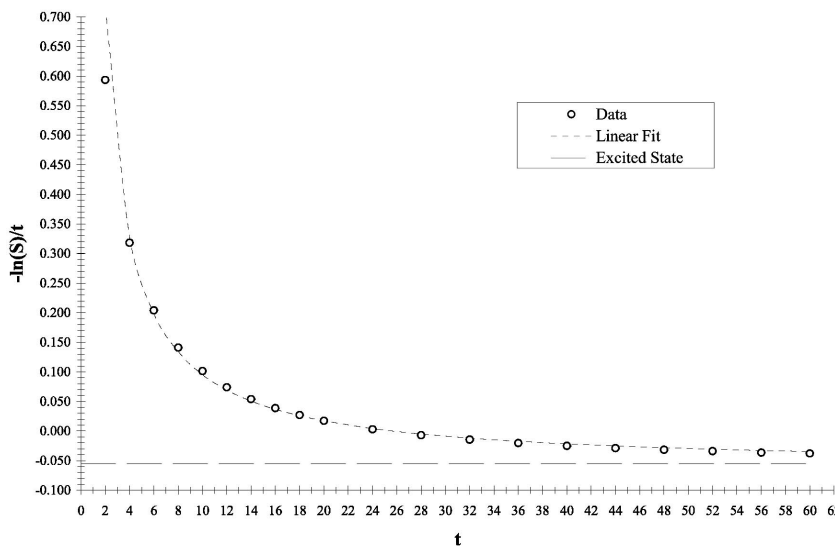


Fig. 7. Plot of $-\ln[\bar{S}(t, \vec{r}_0)]/t$ versus t for the hydrogen $3d_{xy}$ excited state

Fig. 7 shows the results for a random walk simulation implementing the Γ^4 “failure tree” in Fig. 5a. The figure shows a plot of $-\ln[\bar{S}(t, x_0)]/t$ versus t including 1σ error bars and a least square fit using Eq. (10) starting at $t = 4$ with $\ln[C_1] = 0.155608(66)Ut$ and $\lambda_{3d_{xy}} = -0.060610(50)U$. This compares with the lowest Γ^4 symmetry eigenvalue of $\lambda_{3d_{xy}} = -\frac{1}{18} \approx -0.055555 U$. Twenty five million paths were needed to reduce the uncertainty for larger values of t .

As noted above, decreasing the step size Δr and increasing t would result in closer convergence to the exact eigenvalue. These results show that the random walk simulation, using the Feynman-Kac method with imposed “failure tree” constraints results in energy eigenvalues for excited states of the hydrogenic atom.

b. The helium $2^3P_{2,1,0}$ triplet excited state

Consider the helium atom described as two particles with elementary charge and mass M moving in a three-dimensional Coulomb potential defined as

$$V(\vec{r}_1, \vec{r}_2) = -\frac{ke^2}{|\vec{r}_1|} - \frac{ke^2}{|\vec{r}_2|} + \frac{ke^2}{|\vec{r}_{12}|},$$

where k is the Coulomb constant and e is the electron charge. The Schrödinger equation for the system can be written as

$$\left[-\frac{1}{2}\nabla^2(\vec{r}_1, \vec{r}_2) - \frac{1}{|\vec{r}_1|} - \frac{1}{|\vec{r}_2|} - \frac{1}{|\vec{r}_{12}|} \right] \psi(\vec{r}_1, \vec{r}_2) = \lambda \psi(\vec{r}_1, \vec{r}_2), \tag{11}$$

with the unit of energy $U = \hbar^2 / Ms^2$ and $s = \hbar^2 / Mke^2$ the unit of length. One is free at this point to choose operators that form a large number of possible subgroups, each possessing unique symmetry properties. The two configuration space operations $[E, \theta_2]$ defined by

$$E\psi(x_1, y_1, z_1, x_2, y_2, z_2) = \psi(x_1, y_1, z_1, x_2, y_2, z_2)$$

$$\theta_2\psi(x_1, y_1, z_1, x_2, y_2, z_2) = \psi(-x_1, -y_1, -z_1, -x_2, -y_2, -z_2)$$

leave the Hamiltonian invariant and form a group G_1 . The multiplication table and irreducible representations for the group G_1 are shown in Table III. The first few projected eigenfunctions for each irreducible representation of G_1 are shown in Table IV. The helium spectrum has been sorted and classified by the irreducible representations of G_1 . The corresponding “failure tree” is shown in Fig. 8. If Γ^2 symmetry constraints are to be maintained, the whole path must be rejected when either $\theta_2^{-1}\vec{R}$ is also in the path. By this procedure, it is assured that every path that does not fail the symmetry constraints defined by Γ^2 belongs to a configuration space region with that symmetry.

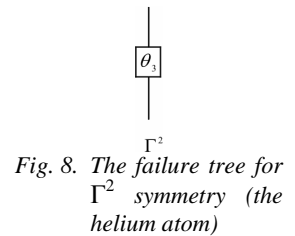


Fig. 8. The failure tree for Γ^2 symmetry (the helium atom)

Table III. The multiplication table and the irreducible representations for the group G_1 (the helium atom)

	E	θ_2		E	θ_2
E	E	θ_2	Γ^1	1	1
θ_2	θ_2	E	Γ^2	1	-1

Table IV. Classification of the first few eigenfunctions for the group G_1 (the helium atom)

	Γ^1	Γ^2
λ_1	$\Psi_{1\ 1s_0}(\vec{r}_1, \vec{r}_2)$	
λ_2	$\Psi_{2\ 3s_1}(\vec{r}_1, \vec{r}_2)$	
λ_3	$\Psi_{2\ 1s_0}(\vec{r}_1, \vec{r}_2)$	
λ_4		$\Psi_{2\ 3p_{2,1,0}}(\vec{r}_1, \vec{r}_2)$
λ_5		$\Psi_{2\ 1p_1}(\vec{r}_1, \vec{r}_2)$

Consider a random walk numerical simulation to the solution of the Schrödinger equation of the helium atom Eq. (11), using the Feynman-Kac method with the imposed “failure tree” constraints defined by Γ^2 irreducible representation. The step size for this system is determined to be

$$\Delta x = \Delta y = \Delta z = \frac{0.529166 \times 10^{-10}}{\sqrt{n}} \text{ meters ,}$$

where $n = 900$. Fig. 9 shows a plot of $-\ln[\bar{S}(t, \vec{r}_0)]/t$ versus t including 1σ error bars for the uncertainty, where $\bar{S}(t, \vec{r}_1, \vec{r}_2)$ is the path integral simulation result as defined in [6]. Four million paths were needed for this convergence. A least squares fit of the data starting at $t = 4$ to the equation $-\ln[\bar{S}(t, x_0)]/t = \lambda_1 - \ln[C_1]/t$ is shown along with the lowest variational result for the eigenvalue. The least square fit yields the values $\ln[C_1] = -0.278(135)Ut$ and $\lambda_{2^3P_{2,1,0}} = -2.139(29)U$. This compares with the variational result for the eigenvalue $\lambda_{2^3P_{2,1,0}} \approx -2.133U$ for Γ^2 irreducible representation [21]. These results confirm that the random walk numerical simulation to the solution of the

Schrödinger equation of the helium atom, using the Feynman-Kac method with imposed “failure tree” constraints associated with Γ^2 irreducible representation results in the energy for the $2^3P_{2,1,0}$ triplet excited state of the helium atom.

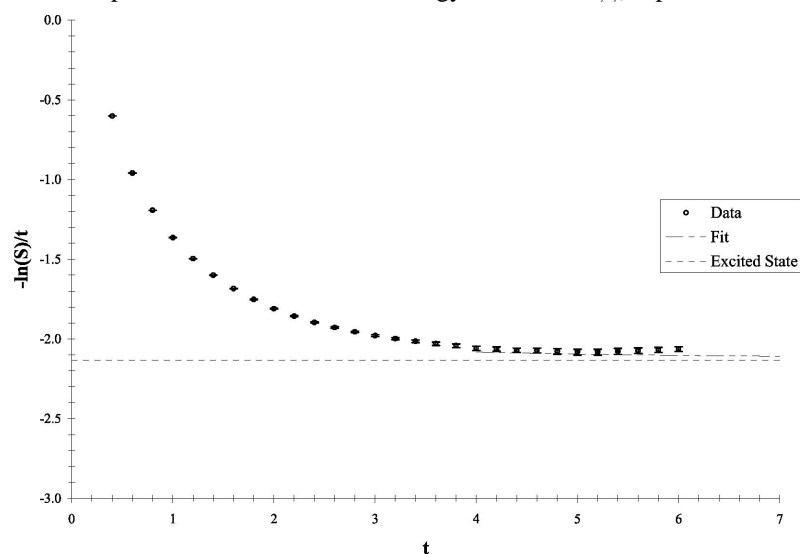


Fig. 9. Plot of $-\ln[\bar{S}(t, \vec{r}_0)]/t$ versus t for the helium $2^3P_{2,1,0}$ triplet excited state

VI. Conclusions

A numerical procedure, the “failure tree” method, for finding solutions of the Schrödinger equation using stochastic methods has been developed. The procedure is based on the use of transformation properties of the irreducible representations of the symmetry group of the Hamiltonian and properties of a continuous path. The “failure tree” method is used to calculate energies of the lowest excited states of quantum systems possessing anti-symmetric nodal regions in configuration space using the Feynman-Kac path integral method. Within the “failure tree” method the symmetry constraints on random walk simulations required to remain interior to a nodal region are obtained. These constraints are associated with a given irreducible representation of a symmetry group of the Hamiltonian and are found by identifying the eigenvalues for the irreducible representation corresponding to symmetric or antisymmetric eigenfunctions for each group operator. Since numerical simulations are reduced to a region of configuration space where the many particle wave function does not change sign, and the sign problem for fermions is never encountered. The method provides exact eigenvalues of excited states in the limit of infinitesimal step size and infinite time.

The “failure tree” method has been applied to compute the eigenvalues of the lowest excited states of the hydrogenic and helium atoms that transform as Γ^2 , Γ^4 and Γ^2 irreducible representations, respectively. A subgroup of configuration space operators has been identified and the “failure trees” have been then constructed based on the antisymmetric properties of each irreducible representation and properties of path continuity. Sufficiency conditions and Boolean logic have been used to simplify the “failure trees”.

The method described by the present work focuses on calculations of excited states with only statistical errors determined by the need to use finite step sizes and time for numerical simulations.

Acknowledgments

This work is dedicated to Boris I. Kochelaev on the occasion of his 70th birthday and supported in part by the Robert A. Welch Foundation.

References

1. P. Exner, *Open Quantum Systems and Feynman Integrals* (Reidel Pub. Co., Boston, 1985) Chapter 5, p. 217.
2. M. Reed and B. Simon, *Methods of Modern Mathematical Physics*, (Academic Press, New York, 1975), Vol. II, pp. 279-281.
3. M.D. Donsker and M. Kac, *Journal of Research National Bureau of Standards* **44**, (1950) 581.
4. A. Korzeniowski, *Statistics and Probability Letter* **8**, (1989) 229.
5. A. Korzeniowski, J.L. Fry, D. Orr and N.G. Fazleev, *Phys. Rev. Lett.* **69**, (1992) 893.
6. J.M. Rejcek, S. Datta, N. G. Fazleev, J.L. Fry and A. Korzeniowski, *Computer Physics Communications* **105**, (1997) 108.
7. B. Simon, *Functional Integration and Quantum Physics*, (Academic Press, New York, 1979).
8. J.B. Anderson, in *Reviews in Computational Chemistry*, Volume 13, Chapter 3, Edited by K. Lipkowitz and D. Boyd (Wiley-VCH, John Wiley and Sons, Inc., New York, 1999), pp. 133-182.
9. M. Caffarel, P. Claverie, C. Mijoule, J. Andzelm and D. Salahub, *J. Chemical Physics* **90**, (1989) 990.
10. W. Lester and B. Hammond, *Annu. Rev. Phys. Chem.* **41**, (1990) 283.
11. D. Ray, *Transactions of the American Mathematical Society* **77**, (1954) 299.
12. D.M. Ceperley and B. Alder, *Science* **231**, (1986) 555.

13. D.M. Ceperley, *Journal of Statistical Physics* **63**, (1991) 1237.
14. E. Lieb and D. Mattis, *Phys. Rev.* **125**, (1962) 164.
15. D.J. Klein and H. M. Picket, *Journal of Chemical Physics* **64**, (1976) 4811.
16. E.B. Wilson, *Journal of Chemical Physics* **63**, (1975) 4870.
17. L.D. Landau and E. M. Lifshitz, *Quantum Mechanics Non-Relativistic Theory*,
18. (Pergamon Press Ltd., Oxford, 1977), p. 59.
19. M.A. Lavrent'ev and L.A. Lyusternik, *The Calculus of Variations*, (2nd edition, Moscow, 1950), Chapter IX.
20. E.P. Wigner, *Group Theory and its Application to Quantum Mechanics of Atomic Spectrum*, (Academic Press Inc.,
New York, 1959), p. 118.
21. Alexei M. Frolov, *J. Phys. B: At. Mol. Opt. Phys.* **36**, 2911 (2003).